ELSEVIER

Cement & Concrete Composites 25 (2003) 625–632

Cement & Concrete Composites

www.elsevier.com/locate/cemconcomp

Reinforcement corrosion and the deflection of RC beams—an experimental critique of current test methods

Y. Ballim *, J.C. Reid

School of Civil and Environmental Engineering, University of the Witwatersrand, Private Bag 3, WITS, 2050 Johannesburg, South Africa

Abstract

This paper presents an experimental critique of the current test methods used to assess the effects of reinforcement corrosion on the serviceability deflections of reinforced concrete beams. Importantly, the work reported here highlights the weakness of tests aimed at assessing the deflection behaviour of beams in which the corrosion of the steel and the application of the service loads are undertaken as two separate and sequential processes.

In the present series of tests, the central deflections of beams subjected to 23% and 34% of the design ultimate load, under 4-point loading subjected to simultaneous accelerated corrosion, were monitored over a period of approximately 30 days. Uncorroded beams were used as control samples and tested in parallel with the corroded samples.

The results show the importance of assessing the structural effects of reinforcement corrosion under simultaneous load and corrosion conditions, as would occur in situ. In this situation, when 6% of the mass of steel is corroded, beam deflections are increased by 40–70% relative to the deflection of the control samples.

Keywords: Reinforced concrete; Corrosion; Durability; Deflection; Serviceability; Accelerated corrosion; Cracking

1. Introduction

Increased cracking and possible bond slippage increases the serviceability deflections of a reinforced concrete (RC) beam which has deteriorated as a result of corrosion of reinforcement. The extent of this increased deflection and the nature of the possible problems that may result are important aspects requiring attention in any assessment of the repair and rehabilitation needs of such a structure. A more general understanding of the relationship between reinforcement corrosion and structural integrity is also necessary to assist owners of large stocks of concrete infrastructure to plan the layout of capital for maintenance and repairs, often in a context of limited financial and human resources.

A number of researchers [1–6] have made important contributions to the development of our understanding of the effects of corrosion on structural performance. Much of this work is laboratory-based and, in order to reduce the testing time, corrosion of the reinforcement is accelerated by impressing an electrical current on the steel. This process is often further hastened by the inclusion of chloride into the concrete at the time of mixing so that, when the corrosion current is applied, the steel is de-passivated and the efficiency of the corrosion current is enhanced. Studies are then carried out on the corroded specimens to monitor the effects of the corrosion on performance aspects such as bond strength, deflection and bending and shear resistance under serviceability and ultimate load-testing conditions. As a model of in situ conditions, this approach has two important drawbacks:

- The process of corrosion of the steel precedes the application of test loads. In real structures, the corrosion takes place while the structure carries load and the two effects act synergistically to accelerate the deterioration of the structure. For example, in the case of a beam element, cracks induced by the corrosion products are widened by the effects of the applied loads (and vice versa) thus allowing greater access to oxygen and water for more rapid corrosion than if the load effects were not simultaneously imposed.

* Corresponding author. Fax: +2711-3391762.
E-mail address: ballim@civil.wits.ac.za (Y. Ballim).

0958-9465/02/$ - see front matter
doi:10.1016/S0958-9465(02)00076-8

- During the corrosion process, the time-dependent effects of a sustained load on serviceability limit state behaviour are not considered. The magnitude of corrosion related stresses and the duration and magnitude of external loads are both influencing factors in the deformation of the structure.

For the research project reported in this paper, it was considered important that a contribution to the understanding of the effects of corrosion on structural performance should be based on an assessment of performance under conditions of carbonation-induced depassivation of the steel followed by simultaneous load and reinforcement corrosion. The project involved the testing of two series of RC beams subjected to reinforcement corrosion while maintaining a sustained load. The test conditions were the same for the two series of tests except that the sustained loads were 23% and 34% of the design load capacity for the Series 1 and Series 2 beams respectively.

This paper also presents a description of a purpose-made load rig and the method by which the corrosion of reinforcement was accelerated. This is followed by a presentation and discussion of the results of tests conducted to characterise the effects of corrosion on structural performance under serviceability loads.

2. Description of the sustained load test rig

A loading rig was developed for this investigation to allow a sustained load to be applied to a simply supported RC beam over a span of 1050 mm, in the 4-point bending load configuration. The load is applied through a compressed spring, onto a load distributor which is placed on the top of the test beam. The underside of the beam and the supports were located inside a galvanised, watertight tank containing an electrolyte (3% NaCl solution) and a steel bar which acts as the cathode for the accelerated corrosion process. The general layout of the load rig is shown in Fig. 1. Six test rigs were fabricated to allow simultaneous testing of three beams subjected to accelerated corrosion and three control beams which were loaded but not subjected to corrosion of the steel.

Compression of the spring was achieved by turning the nuts on the threaded rod above the movable plate and the magnitude of the load was controlled by monitoring the vertical compression of the spring. The springs were fabricated to yield a spring rate of 400 N/mm. For the six springs used in these tests, calibration procedures indicated that the spring rates varied between 381 and 414 N/mm. Using a spirit level to ensure that the movable loading plate was horizontal during loading and a vernier depth gauge, it was possible to compress the spring to an accuracy of 0.1 mm. This translates to a load accuracy of approximately 0.05 kN.

The inside of the galvanised electrolytic tank was sealed and coated with polyurethane sealant. However, the tops of the simple supports were left uncoated as there was some concern that this may allow for deflection of the beam at the supports, resulting in erroneous measurements of the central deflections. In order to eliminate the potential for corrosion of the supports, the I-section beam (onto which the supports were welded) was rendered cathodic by being connected, together with the steel bar cathode in the electrolytic tank, to the negative terminal of the dc power supply source.

For the first series of tests (discussed later), central deflections of the beam were measured using two dial gauges, one placed on each side of the beam. An individual deflection reading was taken as the average of the readings on the two dial gauges. However, at the end of the test, it was found that the tops of the beam supports had corroded and caused the beams to deflect at the support points. Hence, for the second series of tests, additional dial gauges were used to measure the deflec-

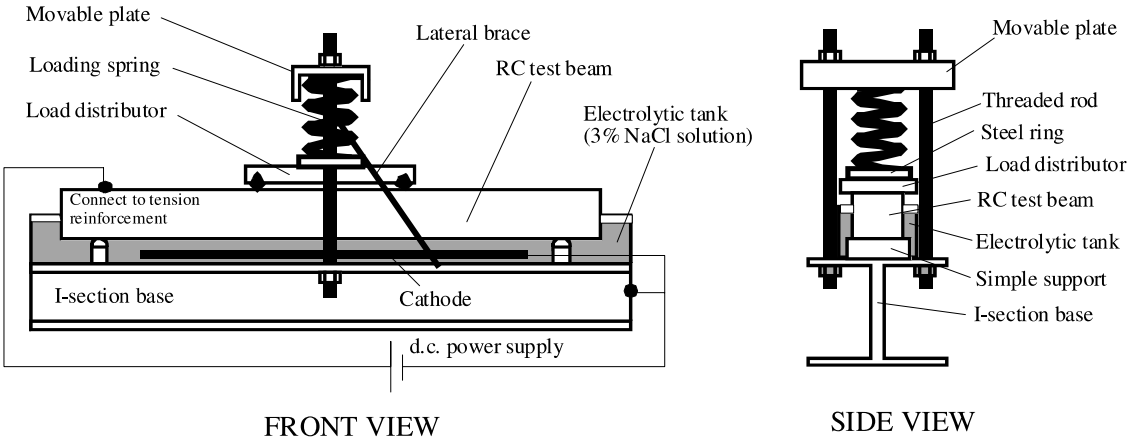

Fig. 1. Schematic arrangement of the sustained load test rig.

tion of the beams at the support points as well. This allowed the central deflection of the beams to be determined relative to that of the supports.

3. Laboratory procedure

3.1. Test beam dimensions and steel reinforcement

Twelve beams were cast with the dimensions and reinforcing layout shown in Fig. 2. The beams were designed to fail in flexure. Design calculations were carried out in accordance with SABS 0100-1 [7]. A single 16 mm N, deformed high tensile steel bar (Y16) was used as the tension reinforcement and 8 mm N, smooth mild steel bars were used for the compression and shear reinforcement. All the steel was obtained from the same steel mill run and a sample of the Y16 bar was tested to give a 0.2% proof stress of 574 MPa.

The shear stirrups were covered with a section of heat-shrink plastic at the points of contact with the main tension steel bar. This was done to electrically isolate the rest of the steel cage from the main tension bar so that the impressed current would cause corrosion of the tension reinforcement only.

3.2. Concrete details

All the beams and other test samples were prepared using the concrete mix proportions shown in Table 1. The water/cement (w/c) ratio was determined from local literature [8] to give a 28-day characteristic compressive strength of 40 MPa. Crushed, graded andesite was used for both the sand and stone fractions of the aggregate. A nominal 13.2 mm stone size was used and the sand fraction had a fineness modulus of 3.29 with a grading which satisfied the local concrete sand grading requirements [9]. At 28 days after casting and under standard curing conditions, samples of this concrete gave an average cube compressive strength of 47 MPa and an average elastic modulus value of 35.5 GPa. The tests for determining elastic modulus were conducted in accordance with BS1881: Part 121 [10].

Table 1
Mix proportions of the concrete used for preparing the beams

Portland cement	428 kg/m^3
Water	225 l/m^3
Sand	790 kg/m^3
Stone	1000 kg/m^3

w/c = 0.53; Slump = 40 mm.

3.3. Preparation of test samples

The investigation involved the testing of two series of beams: one carrying a sustained load of $0.23P_u$ and the other with a load of $0.34P_u$. Each series involved load-testing of six beams, three subjected to simultaneous corrosion of the tension steel and three uncorroded, control beams. Two prisms were also prepared, measuring $160 \times 100 \times 150$ mm, cast in timber moulds and used to monitor the progress of accelerated carbonation of the beams (discussed later).

Before placing the concrete in the beam moulds, the exposed end of a length of insulated electrical wire was soldered to one end of the main tension reinforcement bar. This wire was held in place so that it exited from the top face of the beam. All the concrete samples were moist cured for 28 days at 22 ± 1 °C.

3.4. De-passivation of reinforcement by accelerated carbonation

In order to maximise the rate of steel corrosion, it was decided to de-passivate the main tension reinforcement by accelerating the carbonation of the concrete to the level of the steel. This mechanism of de-passivation was selected in preference to techniques such as the inclusion of chlorides into the concrete at the mixing stage, for the following reasons:

- the hydration characteristics of the cement phase are not affected during the important early stages of hydration;
- compounds such as chlorides are consciously excluded from concrete mixes in practice;

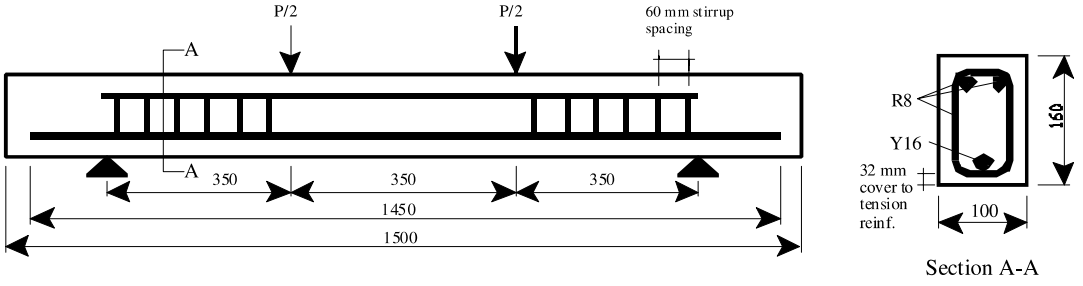

Fig. 2. Dimensions and reinforcement details of the concrete beams tested.

- in inland environments, de-passivation of reinforcement is typically caused by carbonation.

To this end, a simple pressurised carbonation chamber was constructed in which the carbonation of the beams to the depth of the steel could be accelerated. As shown in Fig. 3, the chamber was large enough to accommodate a beam and the two prisms used for monitoring the advance of the carbonation front.

After the 28-day moist curing period, the beams and prisms were placed in a ventilated oven controlled at 50 ± 1 °C for approximately 6 weeks, which was required to ensure a dry and stable moisture condition of the beams. Each beam intended for accelerated carbonation was then placed in a carbonation chamber and, after purging with CO_2, the pressure in the chamber was increased to 80 kPa using the CO_2 pressure cylinder. By monitoring the advance of the carbonation front in the two sample prisms, it was determined that the main tension reinforcing bar had been de-passivated after 6 weeks in the carbonation chamber. At this stage, the beam was removed from the chamber and readied for loading and accelerated corrosion.

3.5. Method of accelerating reinforcement corrosion

A galvanostatic method was used to accelerate the corrosion of the main tension reinforcement bar. This method involved connecting the positive terminal of a dc power supply to the tension reinforcement thus forcing it to become anodic. The negative electrode was then connected to a steel rod (the cathode) placed in the electrolytic solution. The steel rod used as the cathode gave a cathode/anode surface area ratio of 0.7. As mentioned earlier, the negative electrode was also connected to the support beam of the test rig in order to mitigate against corrosion of the support structure.

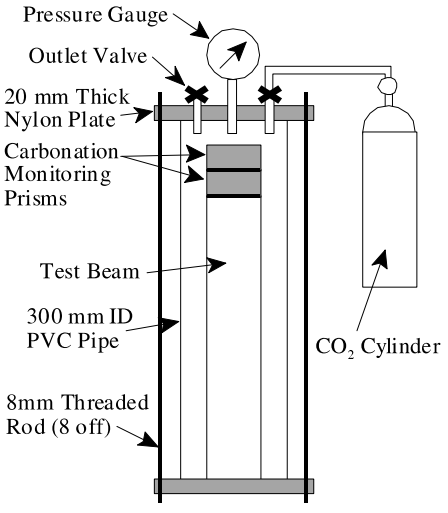

Fig. 3. Schematic arrangement of the accelerated carbonation chamber.

Each corrosion beam had a separate dc power supply with a voltage limit of 30 V and a maximum current output of 3 A. The impressed corrosion current was set to a constant value of 300 mA and this, together with the ohmic potential (resistivity), was monitored daily using a multimeter with an accuracy of 0.01 mA. This corrosion current translated to a current density of approximately 0.4 mA/cm^2.

3.6. Loading procedure

The two groups of beams were placed in the loading rigs with the undersides of the beams approximately 30 mm below the electrolytic solution level (in the case of the corrosion beams) or the water level (in the case of the control, uncorroded beams). The beams were left in this unloaded condition for 24 h, after which the load was applied by compressing the springs to the required level. At this point, a central deflection measurement was obtained. The dc voltage was then applied and both the impressed corrosion current and the spring compression were monitored on a daily basis and adjusted if necessary. Central deflections of both the corroding and the uncorroded beams were also recorded on a daily basis.

After 30 days in the case of the Series 1 tests and 35 days in the case of the Series 2 tests, the beams were removed from the load rigs, inspected for cracking and other visible signs of corrosion damage.

3.7. Quantifying the extent of corrosion

3.7.1. Gravimetric method

At the end of the test programme, the main tension reinforcing bar was carefully removed from each of the corrosion beams and cleaned of all adhering mortar and corrosion product. The bars were then weighed to determine the extent of corrosion. The method used for cleaning the bars was similar to that outlined in ASTM G1-67 [11] and involved brushing the bar with a brass bristle brush and brass wool to remove loosely adhering mortar and corrosion product. The bar was then dipped in a dilute inhibited phosphoric acid solution.

3.7.2. Using Faraday's law

This method was used to determine a theoretical relationship between the time over which the impressed current was allowed to flow and the extent of corrosion [4,12]. Faraday's law can be written as

$$q_t = mnF \tag{1}$$

where q_t is the charge passed through the circuit at time t after the start of the impressed current, m is the number of moles of reactant consumed (or product formed), n is

the number of electrons required to convert reactant to product and F is Faradays constant (96 485 C/mol).

The charge can also be determined by integrating the current, I, with respect to time as follows:

$$q_t = \int I \, dt \tag{2}$$

Assuming that the oxidation of iron to ferrous ions ($Fe \rightarrow Fe^{2+} + 2e^-$) represents the rate determining reaction, combining Eqs. (1) and (2) yields the following equation, from which the mass of corrosion product can be determined at any time during the accelerated corrosion process:

$$m_c = \frac{q_t w}{nF} \tag{3}$$

where m_c is the mass of the original iron consumed (g) and w is the molar mass of the iron (= 55.85 g/mol for Fe). If m_o is the original mass of the uncorroded bar, the percentage corrosion (C_t) is given by:

$$C_t = \frac{100(m_o - m_c)}{m_o} \tag{4}$$

However, in reality, the $Fe \rightarrow Fe^{2+} + 2e^-$ is not the only reaction which takes place at the anode. There are competing reactions and Faraday's law will only give a true reflection of the extent of corrosion if the total number of equivalents which have entered in the reaction are used. Therefore, given the assumption used above, it is necessary to determine the ratio of the charge consumed in the reaction of interest (oxidation of Fe) to the total charge passed. This ratio is referred to as the current efficiency, N [13], and was obtained by comparing the mass of corrosion product determined from the gravimetric method and from Eq. (3) (for the total accelerated corrosion period). This value of N was then used to adjust the extent of corrosion determined using Eq. (3) at various times during the corrosion process.

4. Results and discussion

4.1. Extent of corrosion

The simultaneous load and corrosion of the beams was continued for 30 and 35 days for the Series 1 and 2 tests respectively. Upon removal of the tension reinforcement bar from each beam, the procedure described in Section 3.7 above was used to determine the final extent of corrosion as well as the progress of corrosion during the sustained loading phase. The results of the final extent of corrosion are presented in Table 2. It can be seen that the Series 2 beams, which carried a larger proportion of the ultimate load and a longer period of corrosion, showed higher extents of corrosion. This is probably the result of increased cracking of these beams leading to a higher corrosion current during the accelerated corrosion procedure. The difference between the extents of corrosion determined by the two methods also confirms that, while the $Fe \rightarrow Fe^{2+} + 2e^-$ reaction may be the dominant reaction, it is not the only reaction taking place at the corrosion sites. Furthermore, although a visual assessment showed that this was a small effect, some of the current was "lost" to the corrosion of the support pedestals (discussed later) under the corroded beams.

4.2. Deflection behaviour at the serviceability limit state

Fig. 4a and b show the mid-span deflections of the Series 1 and 2 beams over the period of sustained loading. In the presentation of the results in these figures, the measured deflections of each beam was adjusted so that all the beams gave the same value of initial elastic deflection. For an individual beam, the deflections were normalised to the average of the initial deflections for the six beams. Table 3 shows the maximum, minimum and average initial deflections for the six beams in each of the Series 1 and 2 tests. The reason for the more erratic nature of the Series 1 results is that only central deflection measurements were obtained for this series. These results were therefore distorted by settlement at the supports and, in the case of the corrosion beams, the corrosion of the supports themselves.

As it happened, despite the support beam being connected to the negative terminal of the power source, the supports showed some corrosion upon removal of the beams. This situation was corrected with the Series 2 tests by placing additional deflection gauges on the top of the beams over the supports. This allowed the

Table 2
Extent of corrosion determined from the gravimetric weight loss and Faraday methods

Series	Beam number	% Corrosion (gravimetric)	% Corrosion (Faraday)	Current efficiency N (%)	Average N (%)
1	1	6.38	9.18	69.5	68.1
	2	5.88	9.24	63.6	
	3	6.56	9.23	71.1	
2	1	8.47	11.30	75.0	72.2
	2	5.61	8.06	69.6	
	3	7.98	11.08	72.0	

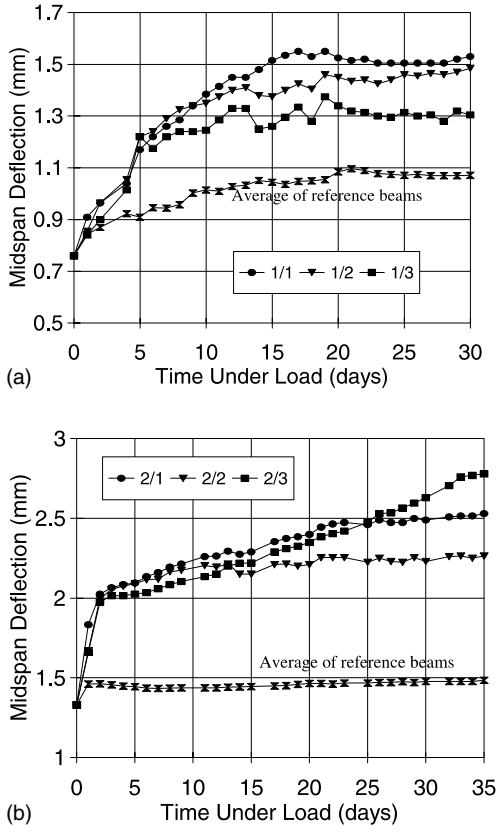

Fig. 4. Adjusted deflection behaviour of (a) the Series 1 beams loaded at $0.23P_u$ and (b) the Series 2 beams loaded at $0.34P_u$.

Table 3
Analysis of initial elastic deflections of the six beams in each test series

Test series	Initial elastic deflection (mm)		
	Maximum	Minimum	Average
1	0.80	0.72	0.76
2	1.39	1.28	1.33

central deflection to be determined relative to the support points.

Fig. 4b also shows that the Series 2 reference beams showed negligible creep and shrinkage effects. Very small creep-induced deflection of the beams is to be expected since the beams were pre-dried before being loaded and the time-dependent, viscous movement of concrete is usually associated with the presence of mobile water in the cement paste [14]. The low moisture content of the beams at the time of loading would account for the low creep deflections observed.

Fig. 4a shows that, after approximately 3 days of loading, the Series 1 corrosion beams showed a significant increase in deflection and this was accompanied by a decrease in the measured ohmic potential (or resistivity). It can be assumed that this was the result of the formation and propagation of a crack on the underside of the beam, linking the electrolyte solution directly to the tension reinforcement bar. Using Faraday's law with the current efficiency correction, it was estimated that the extent of corrosion at this stage of loading was approximately 0.6% by mass of the reinforcing steel bar. However, this relatively small extent of corrosion resulted in a 27% increase in deflection over that of the reference beams. This effect was also noted by Rodriguez et al. [15] who noted crack widths ranging from 0.1 to 0.3 mm after 0.6% corrosion of a 16 mm N reinforcement bar in a concrete beam. They note further that this could explain the significant deterioration in some concrete structures with low measured corrosion rates.

After 5 days of loading, the rate of increase in the deflection of the Series 1 corrosion beams becomes more gradual and this is attributed to

- deterioration of bond at the steel/concrete interface;
- loss of confinement due to widening of longitudinal cracks;
- formation of new flexural cracks and further widening of old ones.

After the load and accelerated corrosion period, the beams were removed from the load rigs and crack maps were prepared for the undersides and vertical sides of each corroded beam in both series of tests. In general, each beam showed a longitudinal crack following the tension steel over most of the underside of the beam. Transverse cracking was concentrated in the constant moment region of the underside of the beams. These cracks generally also reflected up the sides of the beams. While the crack patterns were similar for the Series 1 and 2 beams, the Series 2 beams showed more extensive and wider cracks upon unloading. Significant corrosion staining of the lower ends of the beams was evident and, in the case of the Series 2 beams, some spalling of the concrete cover to the tension reinforcement occurred. It should also be noted that, Okada et al. [16] argue that longitudinal cracks have a very small effect in reducing the structural performance of concrete with corrosion-induced cracking.

The usefulness of such crack maps is limited by the fact that the cracks are viewed after unloading the beams. This means that the cracks are being viewed at a smaller size than when the beams are loaded and small cracks under load may close after unloading and are therefore not mapped. Furthermore, such a crack map gives no indication of the sequence and progression of the cracking. There is clearly a need for techniques to be used which allow the cracking to be monitored over time while the beam is under load and simultaneous steel corrosion.

Fig. 4(b) shows an unusual behaviour for sample 2/2 in that this beam showed little to no increase in deflection after 14 days under load. As is evident from Table 2,

this sample also showed a significantly lower extent of corrosion when compared with the two companion samples. This sample also showed narrower longitudinal cracking on its underside than the other two beams in the Series 2 tests. While this may have been the result of inaccuracy in the placement of the main tension steel, it does indicate the importance of cracking in influencing the rate of corrosion and the deflection under service leads. The issue of cracking and crack patterns clearly requires more attention in tests of this nature.

Fig. 5 shows the results of the two series of tests, expressed as a deflection ratio and plotted against the extent of corrosion calculated using Faraday's Law. The deflection ratio (D_{Rt}) at any time t, is calculated as

$$D_{Rt} = \frac{D_{ct}}{D_{ot}} \tag{5}$$

where D_{ct} and D_{ot} are the average deflections of the corrosion beams and the control beams respectively.

The results of the Series 1 and 2 beams show a distinctly bi-linear character with a significant early increase in deflection as a result of load and corrosion-induced cracking, even at fairly low levels of corrosion. As mentioned earlier, corrosion-induced cracking at low corrosion levels was also noted by Rodriguez et al. [15] and the possibility and extent of such cracking is likely to be dependent on aspects such as member geometry, cover depth, steel bar diameter and amount of reinforcing steel.

Reference to Fig. 4 indicates that the turning point in the rate of mid-span deflection of the corrosion beams occurred at approximately 5 days after loading for the Series 1 beams and after only 2 days for the Series 2 beams, being more heavily loaded. However, Fig. 5 shows that, notwithstanding the magnitude of the applied load, the turning point in the rate of deflection of the beams occurs at a corrosion extent of approximately 0.6%. While this issue requires further investigation, it seems to indicate that, for the samples as tested, the initial cracking induced by the combined effects of load and corrosion cause a rapid increase in deflection until a certain extent of corrosion of the steel. Hereafter, increased cracking and widening of existing cracks progresses in a slower and more stable manner.

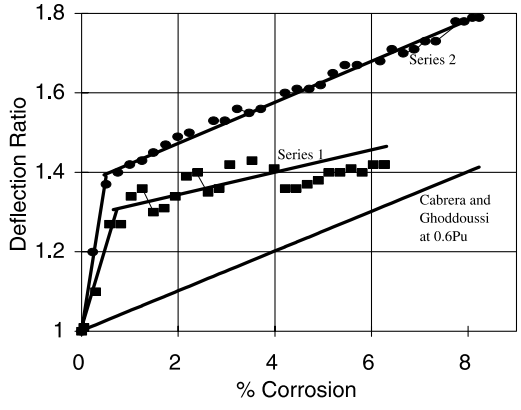

Fig. 5. Effect of extent of corrosion on deflection ratio for the two series of tests.

Fig. 5 also shows the relationship proposed by Cabrera and Ghoddoussi [4], which is of the form:

$$D_{Rt} = 1.002 + 0.05C_t \tag{6}$$

This relationship was established on the basis of tests on beams which were loaded to failure at various extents of corrosion. The deflection ratio was determined with reference to the deflection of a similar, uncorroded beam at a service load of 60% of the ultimate load ($0.6P_u$). Interestingly, the "linear" portion of the Series 2 results very nearly parallel to the Cabrera and Ghoddoussi line. Despite the difference in the level of the applied load, this seems to indicate that the Cabrera and Ghoddoussi line underestimates the deflection ratio largely because it ignores the effect of early cracking under combined load and corrosion conditions. Also, a more detailed analysis of the results obtained by Rodriguez et al. [17] indicates a similar effect. They tested beams in which the steel was corroded before loading and, at an average tension steel corrosion of approximately 16%, the deflection ratio at service load (not defined) is only 1.07. While this is significantly lower than even Cabrera and Ghoddoussi's curve, it does point to the weakness of test methods in which the accelerated corrosion of the reinforcement and the application of load is done sequentially rather than simultaneously.

5. Conclusions

(a) An assessment of the effects of steel corrosion on beam deflections (at the serviceability limit state) which is based on sequential corrosion and load application, results in a significant underestimation of the deflections. This is because the test method does not account for the synergistic effects of simultaneous load and corrosion on cracking of the beam, even at very low levels of corrosion. The results of this investigation show that, in order to better understand the effects of corrosion on structural performance, it is necessary to conduct tests under simultaneous load and corrosion conditions.

(b) It is possible (and, in many cases, preferable) to de-passivate the reinforcing steel by accelerated carbonation and thus avoid the need to include chlorides into the concrete at the mixing stage. However, this does add significantly to the testing time required.

(c) It is necessary to develop a technique which allows the sequence and progression of concrete cracking to be monitored while the beams are loaded and subjected to corrosion. This will add significantly to our understanding of the role of corrosion-induced cracking in increasing the deflection of RC beams.

(d) Under simultaneous load and accelerated corrosion conditions, the time-dependent deflection of the beams increases with progressive corrosion of the reinforcement. A large increase in deflection was noted during the early stages of corrosion as a result of the propagation of transverse cracks on the underside of the beams caused by the flexural tension and the expansive stresses induced by the corrosion products.

(e) For the same extent of corrosion, the deflection ratio increases as the magnitude of the sustained load increases. In the present investigation and at a 6.2% extent of corrosion, increasing the sustained load from $0.23P_u$ to $0.34P_u$ resulted in an increase in the deflection ratio from 1.42 to 1.7.

References

[1] Umoto T, Tsuji K, Kakizawa T. Deterioration mechanism of concrete structures caused by corrosion of reinforcing bars English reprint in Concr Beton, J Concr Soc Southern Africa 1985;38(10):7–12.

[2] Tachibana Y, Maeda K, Kajikawa Y, Kawamura M. Mechanical behaviour of rc beams damaged by corrosion of reinforcement. In: Page CL, Treadaway KWJ, Bamforth PB, editors. Corrosion of reinforcement in concrete. London: Elsevier Applied Science; 1990. p. 178–87.

[3] Al-Sulaimani GJ, Kaleemullah M, Basunbul IA, Rasheeduzzafar. Influence of corrosion and cracking on bond behaviour and strength of reinforced concrete members. ACI Struct J 1990;87(2): 220–31.

[4] Cabrera JG, Ghoddousi P. The effect of reinforcement corrosion on the strength of the steel/concrete bond. In: Proceedings of the Conference on Bond in Concrete Latvia, 1992, CEB, p. 11–24 [chapter 10].

[5] Saifullah M, Clark LA. Effect of corrosion rate on the bond strength of corroded reinforcement. In: Swami RN, editor. Corrosion and corrosion protection of steel in concrete. Sheffield: Sheffield Academic Press; 1994. p. 591–602.

[6] Stanish K, Hooton RD, Pantazopoulou SJ. Corrosion effects on bond strength in reinforced concrete. ACI Struct J 1999;96(6): 915–21.

[7] SABS 0100-1: Code of practice for the structural use of concrete. South African Bureau of Standards, Pretoria, South Africa, 1992.

[8] Addis BJ, editor. Fulton's concrete technology. 6th ed. Halfway House, South Africa: Portland Cement Institute; 1986.

[9] SABS 1083: Specification for aggregates from natural sources. South African Bureau of Standards, Pretoria, South Africa, 1976.

[10] BS1881: Testing concrete. Part 121: Method for determination of static modulus of elasticity in compression. British Standards Institution, London, 1983.

[11] ASTM G1-67: Recommended practice for preparing, cleaning and evaluating corrosion test specimens. American Society for Testing and Materials, Philadelphia, PA, 1971.

[12] Broomfield JP. Assessing corrosion damage on reinforced concrete structures. In: Swami RN, editor. Corrosion and corrosion protection of steel in concrete. Sheffield: Sheffield Academic Press; 1994. p. 1–25.

[13] MacInnes DA. In: The principles of electrochemistry. New York: Reinold Publishing Corporation; 1939. p. 38–9.

[14] Whittmann FH. The effect of moisture content on creep of hardened cement pastes. Rheologica Acta 1970;9(2):282–7.

[15] Rodriguez J, Ortega LM, Gracia AM. Assessment of structural elements with corroded reinforcement. In: Swami RN, editor. Corrosion and corrosion protection of steel in concrete. Sheffield: Sheffield Academic Press; 1994. p. 171–85.

[16] Okada K, Kobayashi K, Miyagawa T. Influence of longitudinal cracking due to reinforcement corrosion on characteristics of reinforced concrete members. ACI Struct J 1988;85(2):134–40.

[17] Rodriguez J, Ortega LM, Casal J, Diez JM. Assessing structural conditions of concrete structures with corroded reinforcement. In: Dhir RK, Jones MR, editors. Concrete repair, rehabilitation and protection. London: E&FN Spon; 1996. p. 65–78.